

# $^{13}\text{C}$ transport studies in L-mode divertor plasmas on DIII-D

S.L. Allen <sup>a,\*</sup>, W.R. Wampler <sup>b</sup>, A.G. McLean <sup>c</sup>, D.G. Whyte <sup>d</sup>, W.P. West <sup>e</sup>,  
P.C. Stangeby <sup>c</sup>, N.H. Brooks <sup>e</sup>, D.L. Rudakov <sup>f</sup>, V. Phillips <sup>g</sup>, M. Rubel <sup>h</sup>,  
G.F. Matthews <sup>i</sup>, A. Nagy <sup>j</sup>, R. Ellis <sup>a</sup>, A.S. Bozek <sup>e</sup>

<sup>a</sup> Lawrence Livermore National Laboratory, P.O. Box 808, 7000 East Avenue, L-637, Livermore, CA 94550, USA

<sup>b</sup> Sandia National Laboratories, Albuquerque, NM 87185-1129, USA

<sup>c</sup> University of Toronto Institute for Aerospace Studies, Toronto, Canada M3H 5T6

<sup>d</sup> University of Wisconsin, Madison, WI 53706, USA

<sup>e</sup> General Atomics, San Diego, CA 92186-5608, USA

<sup>f</sup> University of California, San Diego, La Jolla, CA 92093-0417, USA

<sup>g</sup> FZJ Jülich GmbH/EURATOM Institut für Plasmaphysik, TEC, D-52425 Jülich, Germany

<sup>h</sup> Alfvén Laboratory, Royal Institute of Technology, Association EURATOM-VR, Stockholm, Sweden

<sup>i</sup> EURATOM/UKAEA Fusion Association, Culham Science Center, OX14 3DB Abingdon, UK

<sup>j</sup> Princeton Plasma Physics Laboratory, Princeton NJ 08543-0451, USA

## Abstract

$^{13}\text{CH}_4$  was injected with a toroidally-symmetric gas system into 22 identical lower-single-null L-mode discharges on DIII-D. The injection level was adjusted so that it did not significantly perturb the core or divertor plasmas, with a duration of  $\sim 3$  s on each shot, for a total of  $\sim 300$  T L of injected particles. The plasma shape remained very constant; the divertor strike points were controlled to  $\sim 1$  cm at the divertor plate. At the beginning of the subsequent machine vent, 29 carbon tiles were removed for nuclear reaction analysis of  $^{13}\text{C}$  content to determine regions of carbon deposition. It was found that only the tiles inboard of the inner strike point had appreciable  $^{13}\text{C}$  above background. Visible spectroscopy measurements of the carbon injection and comparisons with modeling are consistent with carbon transport by means of scrape-off layer flow.

© 2004 Elsevier B.V. All rights reserved.

PACS: 52.55.Fa; 52.50.Hf; 52.65.-y

Keywords: DIII-D; Divertor plasma; Re-deposition; Impurity transport

## 1. Introduction and motivation for this experiment, analysis, and modeling

Along with tokamak innovation and core confinement, particle transport is one of the three major re-

search themes of the DIII-D program. Particle transport includes fueling with gas puffing and pellets, and density control with the divertor cryopumps. The study of impurity transport on DIII-D is primarily focused on carbon as nearly all of the plasma facing surfaces are graphite. In particular, we are interested in the flows of carbon, and plasma in the scrape-off layer (SOL) and divertor, and how these are influenced by

\* Corresponding author. Tel.: +1 858 455 4137.

E-mail address: [allens@fusion.gat.com](mailto:allens@fusion.gat.com) (S.L. Allen).

various drifts, including  $E \times B$  and  $B \times \nabla B$  drifts. UEDGE fluid modeling continues to indicate that these drifts are critical for the understanding of particle transport in DIII-D divertor discharges. In turn, deposition regions of carbon may be particularly important for international thermonuclear experimental reactor (ITER), as tritium can be co-deposited with the carbon layers, resulting in a large in-vessel inventory.

The first diverted tokamak experiments using  $^{13}\text{C}$  as a tracer for carbon redeposition were performed on JET [1], ASDEX results are presented in [2]. We present in this paper measurements of carbon deposition using toroidally-symmetric-injected  $^{13}\text{C}$  as a tracer in low power L-mode DIII-D plasmas, and find that most of the deposited  $^{13}\text{C}$  is found inboard of the inner strike point at the divertor plate.

## 2. Experimental method and carbon deposition results

The  $^{13}\text{C}$  injection experiment was preceded by a characterization experiment with  $^{12}\text{CH}_4$  (naturally occurring methane with  $\sim 1\%$   $^{13}\text{C}$ ) injection to establish the required non-perturbative injection levels and also document the background plasma conditions. We established that a flow rate of  $\sim 4.5$  T L/s did not significantly perturb the plasma conditions, e.g. the divertor heat flux did not change during the injection. To enable charge exchange recombination (CER) measurements of core carbon content and ion temperature while minimizing plasma heating, neutral beam ‘blips’ (short duration, low power pulses with longer intervals between pulses) were used on both the setup and main plasma shots. The methane was introduced with a fast valve into three tubes spaced  $120^\circ$  apart toroidally in the upper pumping plenum (with the cryopumps disabled). The conductance of the toroidal plenum was large compared to the exit aperture, which is expected to produce a nearly toroidally-symmetric methane injection into the edge plasma. We also performed radial  $X$ -point scans to characterize the strike point plasma conditions with the divertor Thomson scattering and other divertor diagnostics, adding to the considerable divertor and SOL database of these L-mode plasmas [3].

On the following  $^{13}\text{CH}_4$  injection experiment day, we first re-established reproducible L-mode target discharges and verified that all diagnostics were working. The strike point location and all outer gaps were carefully adjusted to the values established on the setup day. We then purged the gas injection system and connected the  $^{13}\text{CH}_4$  gas bottle. The next 22 plasma shots were completed in sequence with no disruptions or failed discharges. A nearly constant shot cycle was maintained, with a 5-min helium glow discharge between shots. Shown in Fig. 1 is an overplot of L-mode discharges 116243–64: the plasma current  $I_p = 1.1$  MA, central elec-

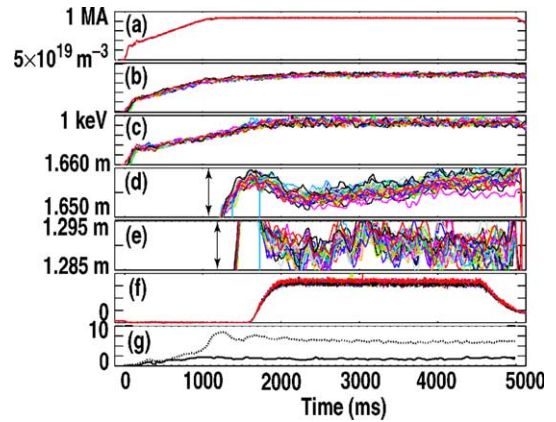


Fig. 1. An overlay of the constant 22 shots 116243–64 (L-mode LSN) used for the  $^{13}\text{C}$  injection experiment. Shown are: (a) plasma current, (b) central density, (c) temperature, (d) outer, (e) inner strike point variation, (f)  $^{13}\text{CH}_4$  injection (pressure in upper toroidal baffle), and (g) outer (dashed) and inner (solid) divertor heat flux from IRTV.

tron density  $n_e \sim 4 \times 10^{19} \text{ m}^{-3}$ , and temperature  $T_e \sim 1.1$  keV were very reproducible. The LSN, low triangularity  $\delta \sim 0.3$  plasma shape was also constant, Fig. 1 shows the variation in the inner and outer strike point locations is on the order of  $\pm 0.5$  cm. The toroidal field was 2 T, with the  $\nabla B$  drift direction towards the lower divertor (‘normal’  $B_T$  for DIII-D). Fig. 1 also shows the consistency of the pressure in the upper pumping plenum during the  $^{13}\text{CH}_4$  injection. The inner and outer heat flux from the IRTV shown in Fig. 1 demonstrates that the divertor conditions are not significantly perturbed by the methane puff (IRTV is data from shot 116254).

These low power L-mode plasmas were typical of DIII-D operation at this density; the inner strike point is detached, the outer attached. Fig. 2 shows these conditions: the divertor plate heat flux profile shows the absence of a well-defined peak at the inner strikepoint, and a well-defined peak in heat flux at the outer strike point, along with a larger ion saturation current from the Langmuir probes. Detailed analysis of these shots, sometimes referred to as ‘Simple as Possible Plasmas’, are presented elsewhere [4], along with UEDGE fluid modeling [5].

At the conclusion of the shot series, we verified that a total of  $\sim 315$  T L of  $^{13}\text{CH}_4$  or  $1.0 \times 10^{22}$  atoms of injected  $^{13}\text{C}$  was injected during the flat-top part of the discharge, both by the change in the supply bottle pressure (330 T L) and by integration of the real-time pressure measurements ( $\sim 300$  T L at plasma flattop,  $\sim 30$  T L in rampdown). We also puffed  $^{13}\text{CH}_4$  into the empty vessel and the RGA mass spectrum (new peak at mass 17) verified that the methane contained  $^{13}\text{C}$ . The usual

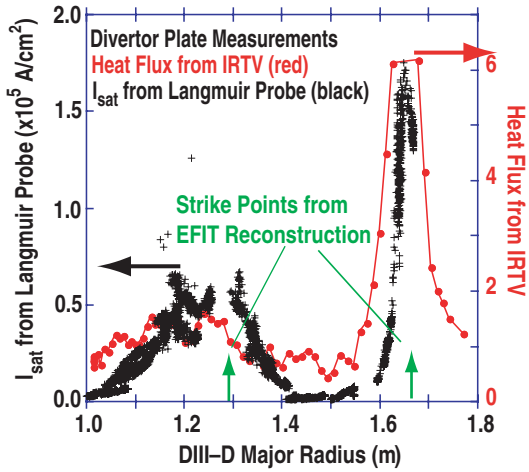


Fig. 2. Typical divertor plate parameters for these discharges, the IRTV (scale right) and ion saturation current (scale left) are consistent with an attached outer divertor and a detached inner divertor. The strike point locations from EFIT at the plate are at 129 and 165.5 cm.

post-campaign processing, such as baking was not performed after this experiment. After the normal safety surveys were performed, the 29 tiles were removed before

any other tasks were started in the vessel. In nearly all cases, it was possible to remove the tiles without touching the plasma-facing surface. Small, localized wipes were taken for health-physics samples before shipping.

These tiles were located both in the divertor and main chamber, as illustrated in Fig. 3. The tile set included 23 tiles distributed poloidally in a narrow band extending only 20° toroidally, as well as 6 from other toroidal angles to check toroidal symmetry and to measure plasma limiters. Note that several tiles near the injection region were also removed for analysis. The tiles were individually packed and transported to Sandia National Laboratory, Albuquerque, NM for analysis. In passing, as shown in the lower inset in Fig. 3, tritium (from years of D–D plasma operation) was found at the base of Tile 8 during health physics surveys of the tiles. This is the only row of tiles that are not interconnected, and demonstrates how tritium can be trapped in layers away from the main plasma-facing surfaces.

The 29 tiles were analyzed by a nuclear reaction analysis (NRA) technique described in detail in Ref. [6]. An analysis beam of 2.5 MeV  $^3\text{He}$  was directed onto the tiles, and energy spectra of charged particles from resulting nuclear reactions  $^{13}\text{C}(^3\text{He},\text{p})^{13}\text{N}$  were recorded. A schematic of the detection geometry is shown in Fig. 4(a); a special sample chamber was used to handle the

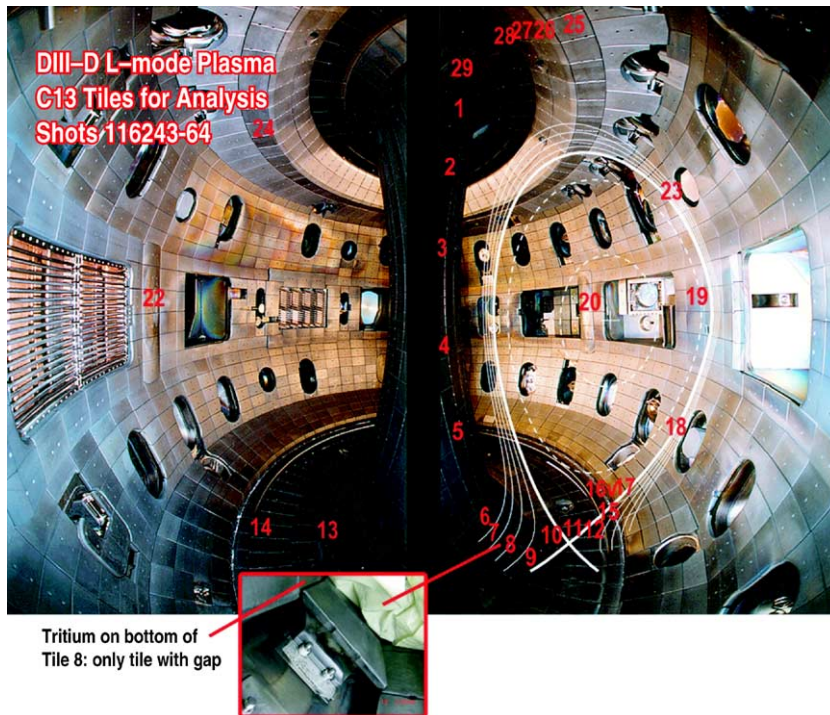


Fig. 3. The location of the 29 tiles removed for  $^{13}\text{C}$  analysis. The lower inset of Tile 8 reveals the gap between it and the centerpost, where tritium (from years of D–D plasma reactions) was measured on the bottom of the tile. All other adjacent tiles are overlapped.

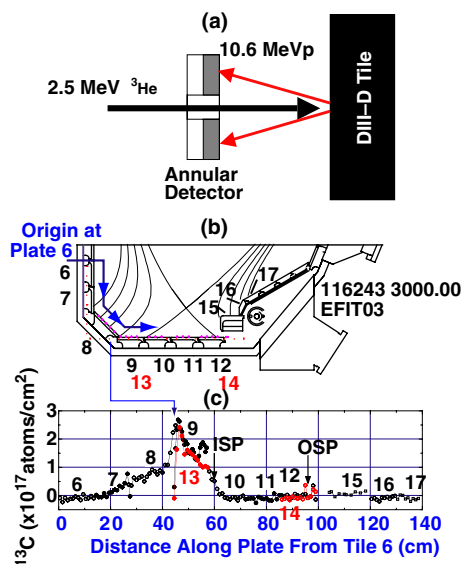


Fig. 4. Results reprinted from Ref. [5]: (a) the setup for the NRA measurements of  $^{13}\text{C}$ , (b) the locations of the tiles, and (c) the  $^{13}\text{C}$  is observed inboard of the inner strike point, primarily Tile 9. The origin of this plot is at the edge of Tile 6. Tiles 9 and 13 and 12 and 14 are at different toroidal locations (Fig. 3), and show similar  $^{13}\text{C}$  concentrations. (For interpretation of the references in color in this figure legend, the reader is referred to the web version of this article.)

large DIII-D tiles. Three measurement scans were made on each tile, with a measurement spacing of  $\sim 1$  cm on each scan, resulting in over 30 points for each tile and 1250 points for all 29 tiles. This technique also measures deuterium, boron and  $^{12}\text{C}$  content in the near-surface region of the tiles; these results are presented in Ref. [6].

The NRA data showed that only the region inboard of the inner strike point had significant deposition of  $^{13}\text{C}$ . Shown in Fig. 4 (reproduced from Fig. 3 in Ref. [6]) is the  $^{13}\text{C}$  density as a function of position for the lower divertor. The abscissa of the plot is the distance along the divertor plate starting at Tile 6 on the inside of the machine. Tiles 8 and 9, which were inboard of the plasma strike point, have the largest  $^{13}\text{C}$  concentration. The large decrease in  $^{13}\text{C}$  at the outboard edge of Tile 9 is due to shadowing by an adjacent tile. All of the other tiles, 1–5, and 10–29 had no detectable  $^{13}\text{C}$  density above the measurement threshold.

Fig. 4 also shows a high degree of toroidal symmetry in the  $^{13}\text{C}$  deposition. Tile 13 (red) is plotted on top of Tile 9, and the data agrees well, even the characteristic drop at the shadowed region of the tile is reproduced. The other comparison is Tiles 12 and 14, which both have low values.

Assuming toroidal symmetry, a simple integration of Fig. 4 yields the total deposition of  $^{13}\text{C}$  particles, which

is  $\sim 35\%$  of the injected  $^{13}\text{C}$ . The remaining  $^{13}\text{C}$  is possibly explained by several different effects. The upper Tiles 25–29 near the injection region did not have measurable  $^{13}\text{C}$ , however, if this large area of the machine were uniformly covered at the estimated detection limit, we would estimate that nearly half of the injected  $^{13}\text{C}$  could be in this region. This is consistent with a 40% local deposition near the inject point predicted by modeling of methane breakup [7], with an areal density below the detection limit. Another possible explanation for the missing  $^{13}\text{C}$  is that the DIII-D machine is pumped down between shots, so some of the  $^{13}\text{C}$  remaining as a gas could be removed during this time. In addition, a 5-min helium glow discharging cleaning cycle was used between shots, although estimates indicate that this low-energy flux would not be very effective at removing the deposited  $^{13}\text{C}$ . We are currently examining the detailed particle balance, including the 21 amu signal from the RGA during the day.

### 3. Comparisons with models

The  $^{13}\text{C}$  was found inboard of the inner strike point for these L-mode LSN plasma shots. In order to understand the important physical processes involved in the deposition process, both heuristic or analysis mode modeling of an assumed entrainment in a flow parallel to  $B_{\text{total}}$  and first principle, fluid mode (UEDGE) calculations have been performed. In the former approach, detailed hydrocarbon breakup calculations with DIVIMP [7] have been compared with 2-D reconstructions of CII and CIII emissions near the injection port. A prescribed ‘counterclockwise’ flow of  $M \sim 0.4$  towards the inner strike point is most consistent with the data. OEDGE and DIVIMP modeling of the  $^{13}\text{C}$  distribution at the inner strike point also is consistent with a flow of  $M \sim 0.4$  [8]. However, the UEDGE calculations (from Braginskii equations) show a more complicated flow pattern for the carbon, particularly at the inner divertor. While UEDGE calculations show a poloidal flow at the top of the plasma, it is primarily from a  $E_r \times B_T$  drift near the separatrix. It is not clear whether the main channel for carbon migration to the inner strike point is the ‘short way’ (through the private flux region, and influenced by  $E \times B$  drifts), or the ‘long way’ (through the top of the machine), as suggested by the ‘analysis mode’ modeling. Future experiments, such as reversing the direction of some of these drifts (by reversing the direction of the toroidal magnetic field) could be used to test the importance of these terms. Direct measurement of the plasma and impurity flow, along with more sensitive measurements of  $^{13}\text{C}$  and detailed exhaust (RGA) measurements, would greatly increase our confidence in scaling the physics in these types of experiments to the possible tritium inventory issue on ITER.

**Acknowledgments**

Work supported by the US Department of Energy under W-7405-ENG-48, DE-AC04-95ER85000, DE-FG03-96ER54373, DE-FC02-04ER54698, DE-AC02-76CH03073, and DE-FG02-04ER54758.

**References**

- [1] J. Likonen et al., *Fus. Eng. Des.* 66 (2003) 68.
- [2] E. Vainonen-Ahlgren et al., these Proceedings. doi:10.1016/j.jnucmat.2004.08.028.
- [3] P.C. Stangeby et al., *J. Nucl. Mater.* 313–316 (2003) 883.
- [4] S. Lisgo et al., these Proceedings. doi:10.1016/j.jnucmat.2004.09.055.
- [5] G.D. Porter, private communications, May 2004.
- [6] W.R. Wampler, these Proceedings. doi:10.1016/j.jnucmat.2004.10.124.
- [7] A.G. McLean, these Proceedings. doi:10.1016/j.jnucmat.2004.10.130.
- [8] S. Elder, these Proceedings. doi:10.1016/j.jnucmat.2004.10.138.